Automated Liver Stiffness Measurements with Magnetic Resonance Elastography

Bogdan Dzyubak[1], Kevin Glaser[2], Meng Yin[2], Armando Manduca[2], and Richard Ehman[2]

[1]Mayo Graduate School, Mayo Clinic, Rochester, Minnesota, United States, [2]Radiology, Mayo Clinic, Rochester, Minnesota, United States

Objective: Magnetic Resonance Elastography (MRE) [1] is an MRI technique that is being increasingly adopted in clinical practice to non-invasively detect and assesss hepatic fibrosis - a relatively common condition [2]. MRE measures stiffness by imaging and analyzing shear wave propagation throughout the liver. Currently, stiffness measurements are made by analysts manually drawing regions of interest, which is a time-consuming technique with inherent variabilities. The goal of this study was to develop an algorithm to provide these stiffness measurements automatically and yield results consistent with trained readers of MRE images.

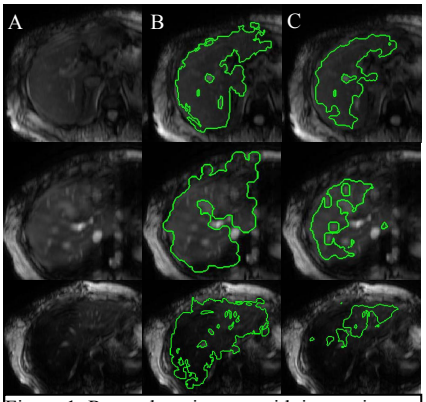

Figure 1: Rows show images with increasing artifact. Columns show original image (A), liver segmentation (B) and processing mask (C).

Method: ***Dataset****:* Gradient-echo MRE images of 96 patients from our database, obtained in compliance with our institutional review board, comprised a training set. All of them were analyzed by Reader 1, with 5 years of experience, and a subset of 57 images by Reader 2 with 6 months of experience. The algorithm was then tested on a new set of 51 images, read by Reader 3 with 3 years of experience. Fig. 1 shows MRE MR magnitude images from 3 cases with various artifacts and image quality.

Initialization*:* Liver segmentation was initialized using an adaptive threshold. The intensity histogram contained two major peaks due to the air and liver. The histogram was thresholded between the peaks and at 50% of the liver peak. This yielded a mask containing the majority of the liver and some other structures (Fig. 2). The resulting mask was cleaned via morphological operations, including: erosions to recede from liver edges, opening and exclusion of all objects except the largest, and hole filling. If the liver peak was not detectable due to significant blurring of the image or signal dropout, initialization was attempted based on an adjacent slice. In case of failure, a predefined contour, with location and size based on the training set was used to initialize the image. Default initialization was used in at least one slice of 14/96 images in the training set and 10/51 images in the test set.

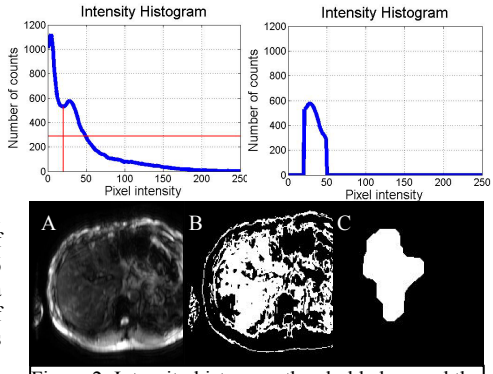

Figure 2: Intensity histogram thresholded around the liver peak to leave an approximate liver shape. Original image (A), thresholded mask (B), morphologically cleaned mask (C).

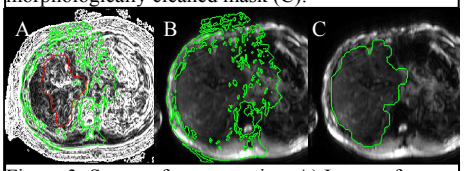

Figure 3: Stages of segmentation. A) Image of gradient normalized by intensity with initialization (red) and segmentation (green), B) preliminary segmentation over original magnitude image, and C) final liver mask after morphological cleaning.

Segmentation*:* The initial contour was expanded with a level set method to find the edges of the liver. The expanding force is created by the lower variance in the internal region of the contour relative to the variance of the external region. The contour adds a pixel (P) if it is similar to the normalized mean of the interior or flows around it if it is more similar to the exterior [3]. This formulation was run on the calculated gradient (G) of the magnitude image normalized by intensity (I) at every point. Within the liver, G≈0 and the contour expands easily. The edges have very high G and medium I, so the contour is stopped. In cases of unpredictably changing ratio, such as borders between organs of similar intensities or the region around the patient that has G≈0 and I≈0, the value of G/I is desirably erratic. The mask created by the level set method is morphologically eroded, first with a small element (which removes the erratic areas), and then, after hole filling, with a large element which pinches leakage areas and excludes regions with many blood vessels. The different stages of segmentation are shown in Fig. 3.

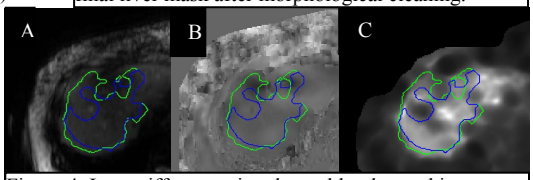

Figure 4: Low stiffness region due to blood vessel is excluded by the reader (blue) but not basic segmentation. Magnitude (A), phase (B), and stiffness (C) images are shown.

Confidence Map and Stiffness*:* The inversion algorithm used to calculate stiffness outputs a confidences map based on fitting a polynomial to an 11x11 processing window. Areas with confidence below 95% are excluded from the manual and automated stiffness measurements. Additionally, because the liver is homogeneous and fibrosis is a diffuse disease, the stiffness image was thresholded for outliers by removing stiffness values with less than 20% of the stiffness mode frequency from the histogram. A similar procedure is done by the readers to exclude tumors or hot spots caused by oblique wave propagation as well as cold spots caused by blood vessels (Fig. 4).

Measurements*:* Mean stiffness for all slices was calculated for every patient. The algorithm's measurement was compared to Reader 1 in the 96 cases, to Reader 2 in the subset of 57 cases, and to Reader 3 in the test set using the Bland Altman test (Fig.5) and intraclass correlation coefficient (ICC).

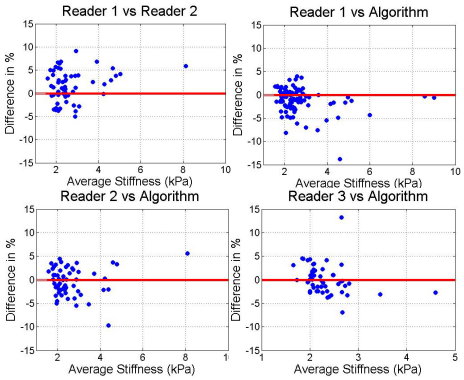

Figure 5: Bland-Altman plots comparing readers to each other and the algorithm to readers.

Results: The range of liver stiffnesses was 1.54 to 9.06 kPa in the training patient cohort and 1.6 to 4.72 kPa in the test cohort. The Bland-Altman comparison of Reader 1 and 2 yielded a bias of -3.4% and a 95% confidence range of ± 13.0%. The algorithm and Reader 1 differed by -2.47 ± 10.5%, while the algorithm and Reader 2 (less experienced) by -0.71 ± 11.8%. In the test set, the algorithm and Reader 3 differed by 0.23 ± 12.5%. The ICCs with a p-value of 0.05 were 0.988 for Reader 1 and 2, 0.993 for Reader 1 and algorithm, 0.99 for Reader 2 and algorithm, and 0.971 for Reader 3 and algorithm (test set). On average, the algorithm took 200 s to process a 4-slice exam on a desktop PC.

Conclusions: The proposed algorithm for automatically determining liver stiffness was found to be fast and highly reliable, even though MRE images can have motion and other signal artifacts present. Its deviation from the readers was comparable to the difference between the readers. Additionally, it performed well on the test set showing robustness to reasonable changes in image parameters. The algorithm can be adapted to MRE data collected using other imaging sequences (e.g., spin echo, EPI) though this may require a separate training set. This algorithm will be beneficial for streamlining the processing of MRE liver images. Future work largely involves specific detection and removal of areas that produce stiffness hot and cold spots.

References: [1] Yin, M., et al., *Assessment of hepatic fibrosis with magnetic resonance elastography.* Clin Gastroenterol Hepatol, 2007. **5**(10): p. 1207-1213. [2] Bataller, R. and D.A. Brenner, Liver fibrosis. J Clin Invest, 2005. 115(2): p. 209-18. [3] Malcolm, J., et al., *Fast approximate surface evolution in arbitrary dimension*, in *Medical Imaging: Image Processing*, J.M. Reinhardt and J.P.W. Pluim, Editors. 2008.